

## Supporting Information

### Flexible and highly fluorescent aromatic polyimide: design, synthesis, properties, and mechanism

Zhuxin Zhou, Yi Zhang\*, Siwei Liu, Zhenguo Chi, Xudong Chen, and Jiarui Xu

PCFM Lab, GD HPPC Lab, Guangdong Engineering Technology Research Center for High-performance Organic and Polymer Photoelectric Functional Films, State Key Laboratory of Optoelectronic Materials and Technologies, School of Chemistry and Chemical Engineering, Sun Yat-sen University, Guangzhou 510275, China; E-mail: [ceszy@mail.sysu.edu.cn](mailto:ceszy@mail.sysu.edu.cn)

#### List of Contents for Supplementary Materials:

Materials and Instrumentation .....	2
Fig. S1 <sup>1</sup> H NMR and <sup>13</sup> C NMR spectra of the intermediates .....	3
Fig. S2 <sup>1</sup> H NMR and <sup>13</sup> C NMR spectra of the diamine monomers .....	4
Fig. S3 FT-IR spectra of polyimide films .....	5
Fig. S4 <sup>1</sup> H NMR spectra of polyimides TzODPI and PyODPI .....	5
Fig. S5 WAXD patterns of the polyimide films .....	6
Fig. S6 Polyimides thermal properties: DSC, DMA, TMA and TGA curves .....	6
Fig. S7 Transmission spectra of polyimide films .....	7
Fig. S8 Absorption spectra of polyimide spin-coated films .....	7
Fig. S9 The chemical structures of model basic units (MBU) TzM and PyM .....	7
Fig. S10 Cyclic Voltammograms of polyimides in NMP .....	7

## Materials and Instrumentation

**Materials.** 4-Nitrobenzoyl chloride, chlorotriphenylmethane, aniline, phosphorus pentachloride ( $\text{PCl}_5$ ), hydrazine monohydrate, tin chloride dihydrate ( $\text{SnCl}_2 \cdot 2\text{H}_2\text{O}$ ), and *N*-methyl-2-pyrrolidone (NMP) were purchased from Aladdin and used as received. 4,4-Oxydiphthalic anhydride (ODPA) purchased from J&K Chemical Ltd., was recrystallized from acetic anhydride and heated at 150 °C under vacuum for 12 h before use. Tetrabutylammonium perchlorate (TBAP) and ferrocene were obtained from Alfa Aesar and used as received. *N,N*-dimethylformamide (DMF) purchased from Aladdin was dried over calcium hydride for 12 h and distilled under reduced pressure. Anhydrous toluene was obtained by distillation and stored over 4A molecular sieves. All other reagents were analytical grade and used as received from commercial sources, unless otherwise mentioned.

**Instrumentation.**  $^1\text{H}$  NMR and  $^{13}\text{C}$  NMR spectra were recorded on a Varian Mercury-plus 300 spectrometer and a Varian Unity Inova 500 NB spectrometer, respectively. All samples were measured in a solution of deuterated dimethyl sulfoxide ( $\text{DMSO-}d_6$ ) with tetramethylsilane (TMS) as an internal standard. Mass spectra were performed on a Thermo EI mass spectrometer (DSQ II). Elemental analysis was run in a CHNS elemental analyzer. Infrared spectra (IR) were analyzed by a BRUKER TENSOR 27 Fourier-transform infrared (FT-IR) spectrometer. The inherent viscosities ( $\eta_{\text{inh}}$ ) of the polyimides were obtained at a solid content of 0.5 wt% in NMP at 30 °C on an Ostwald viscometer. Wide-angle X-ray diffraction (WAXD) measurements were performed on a Rigaku SmartLab X-ray diffractometer at a scanning rate of 10 °/min. Ultraviolet-visible (UV-vis) absorption spectra were obtained on a Hitachi UV-Vis spectrophotometer (U-3900). The PI solution spectra were measured at a concentration of approximate  $2 \times 10^{-2} \text{ mg} \cdot \text{mL}^{-1}$  before the absorbance was normalized. The fluorescence excitation/emission spectra of PI solutions at a concentration of approximate  $2 \times 10^{-2} \text{ mg} \cdot \text{mL}^{-1}$  were recorded using a Shimadzu RF-5301PC spectrometer. The excitation spectra were obtained by detecting the fluorescence intensities at the peak wavelength of the emission spectra, while the emission spectra were obtained with excitation at the peak wavelength of the corresponding excitation spectra. The photoluminescence life time ( $\tau$ ) of the PI film was obtained by a HORIBA integrated spectrometer. The photoluminescence quantum yield ( $\Phi_{\text{PL}}$ ) of the diamine monomers, the PI solutions and thin films on quartz were calculated by using a calibrated integrating sphere coupled to an Edinburgh Instrument Ltd. FLS980 spectrometer. Samples were excited at the wavelength of corresponding excitation peak. Thermogravimetric analyses (TGA) were carried out on a TA thermal analyzer (Q50) under a nitrogen atmosphere at a heating rate of 20 °C/min. Differential scanning calorimetry (DSC) curves were obtained with a NETZSCH thermal analyzer (DSC 204) at a heating rate of 10 °C/min under a nitrogen flow. The dynamic mechanical (DMA) spectra were determined by a TA DMA 2980 analyzer in tensile mode at an amplitude of 20  $\mu\text{m}$ , a preload force of 0.01 N and a force track of 125% at a heating rate of 5 °C/min. Thermomechanical analyses (TMA) were conducted with a TA TMA Q400 analyzer at a preload force of 0.05 N and a heating rate of 10 °C/min. Cyclic voltammetry (CV) measurements were performed on a Shanghai Chenhua electrochemical workstation (CHI660C) using a three-electrode cell in 0.1 M solution of TBAP in *N*-methyl-2-pyrrolidone (NMP) with a Pt disk working electrode, a Ag/AgCl, KCl (sat.) reference electrode, and a glass carbon counter electrode. All measurements were performed under an inert argon atmosphere at a scanning rate of 50 mV/s. A solution of ferrocene (5 mM) was used as an external reference for calibration.

Molecular simulation and analysis were carried out with the Gaussian 09 and the Multiwfn program package. The molecular geometry, molecular orbitals and dipole moment of the basic unit in the polyimide molecular structure were calculated and optimized by means of the density functional theory (DFT), using the Becke's three-parameter hybrid density functional method in conjunction with Lee-Yang-Parr's correction functional (B3LYP) method, and the 6-31+G(*d*) basic set. For all simulations, vibration frequencies were calculated analytically to ensure the minimum total energy of the optimized molecular geometry.

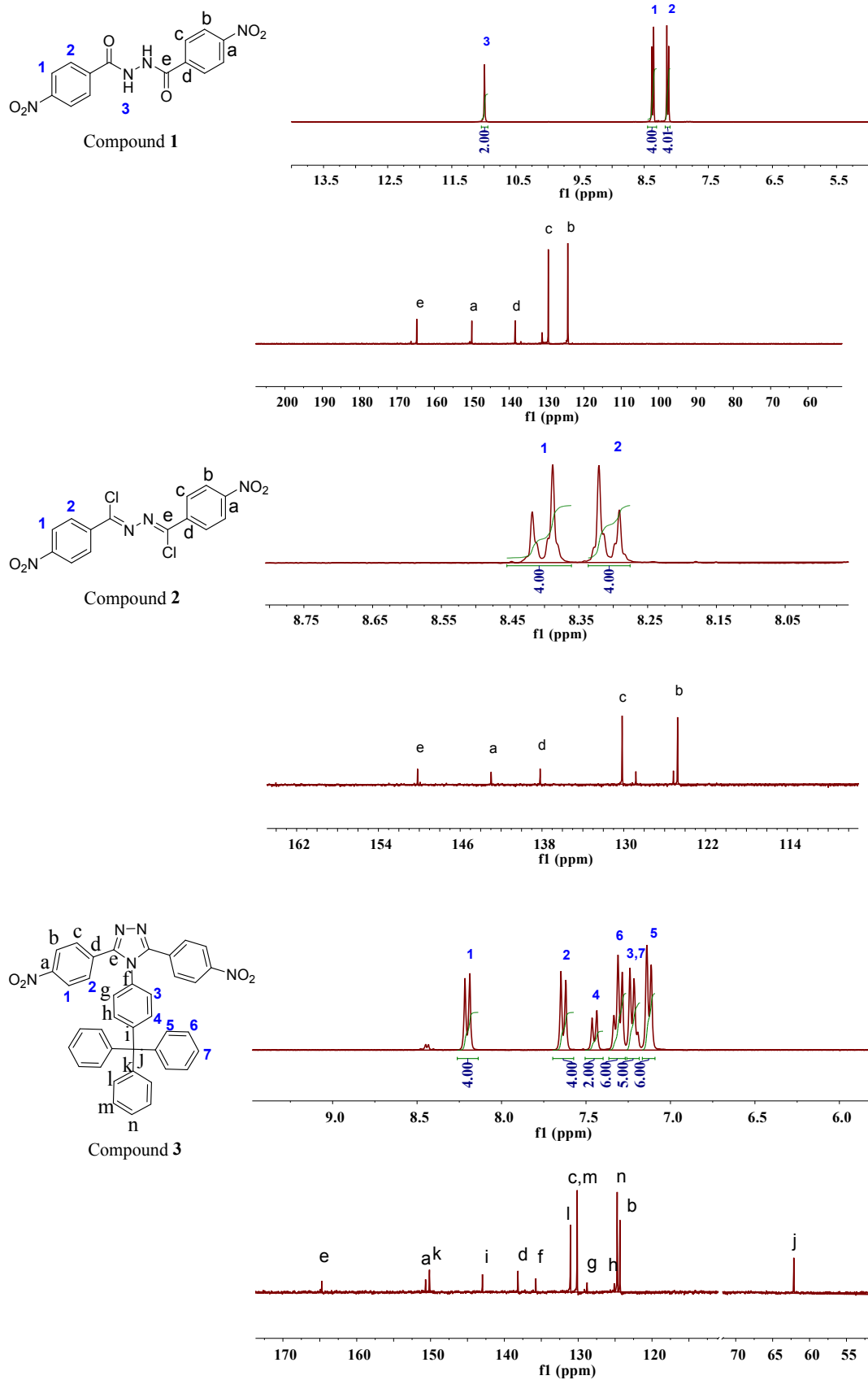


Fig. S1  $^1\text{H}$  NMR and  $^{13}\text{C}$  NMR spectra of the intermediates

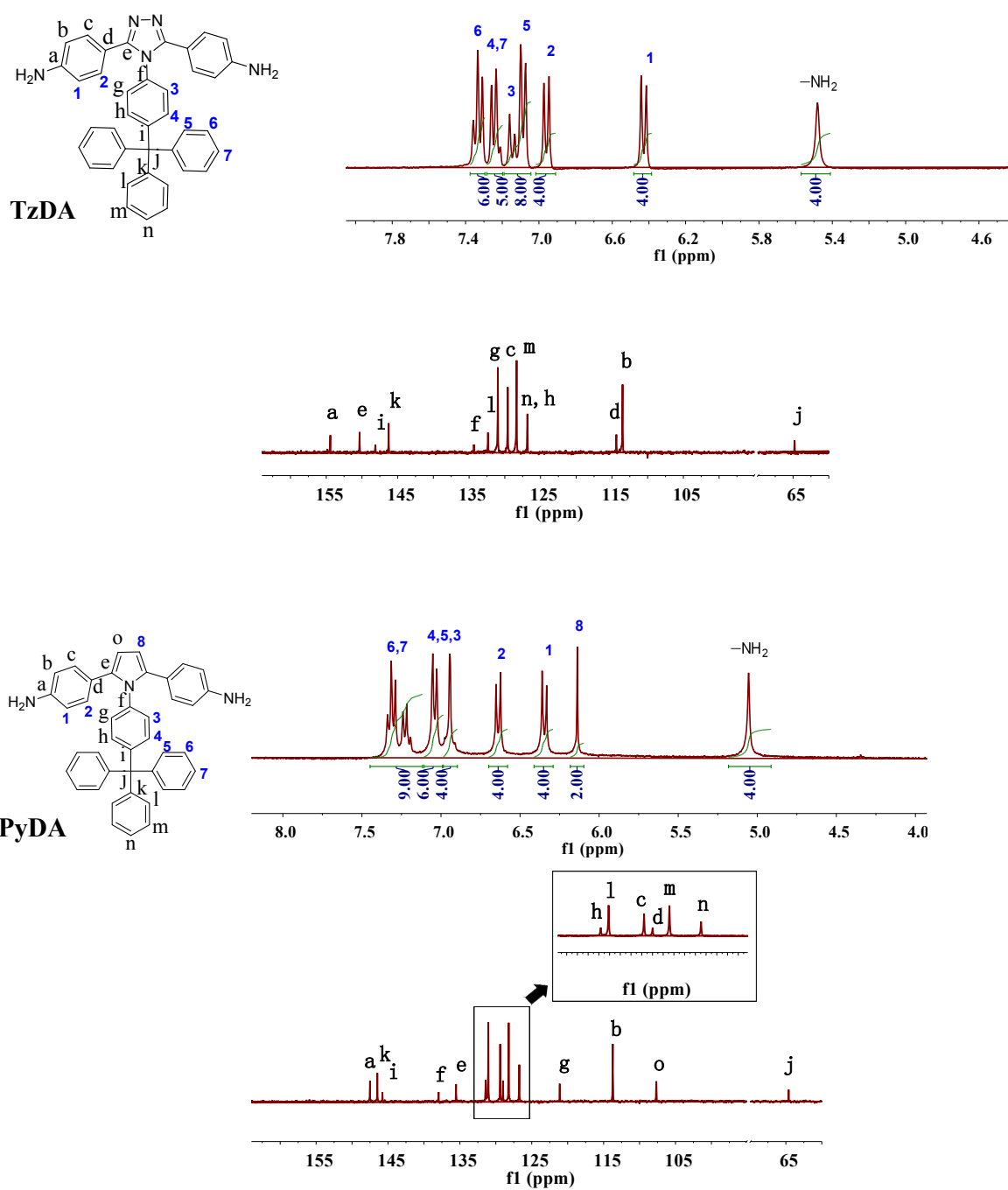


Fig. S2  $^1\text{H}$  NMR and  $^{13}\text{C}$  NMR spectra of the diamines monomers

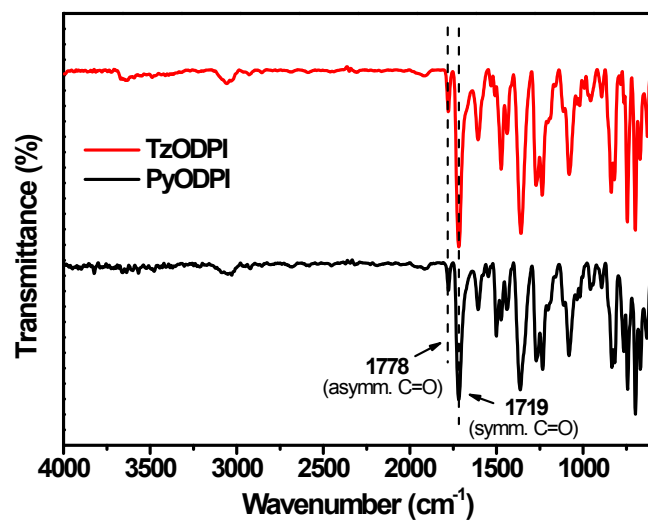


Fig. S3 FT-IR spectra of polyimide films

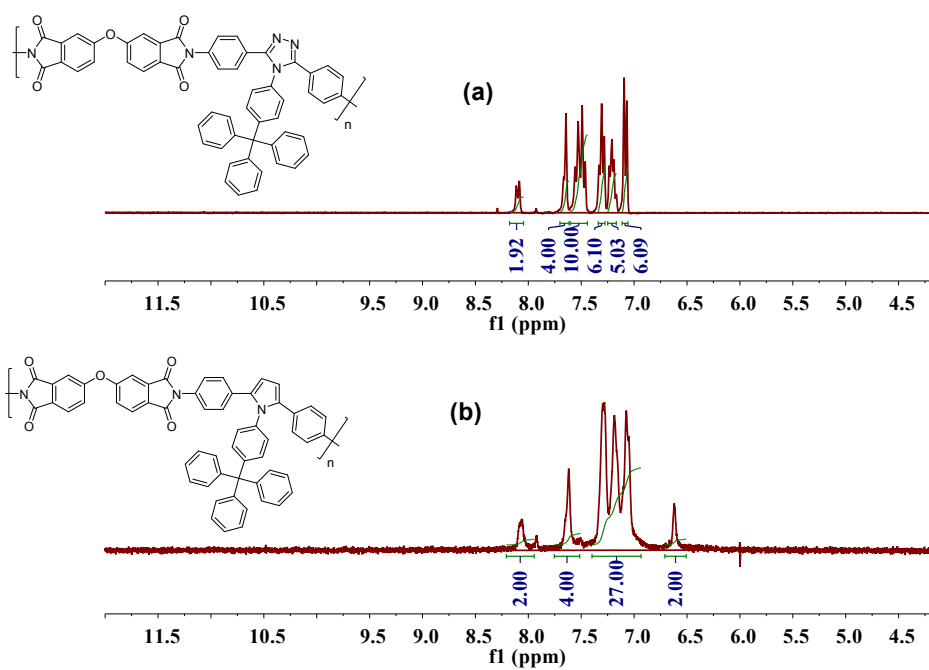


Fig. S4  $^1\text{H}$  NMR spectra of polyimides (a) TzODPI, and (b) PyODPI

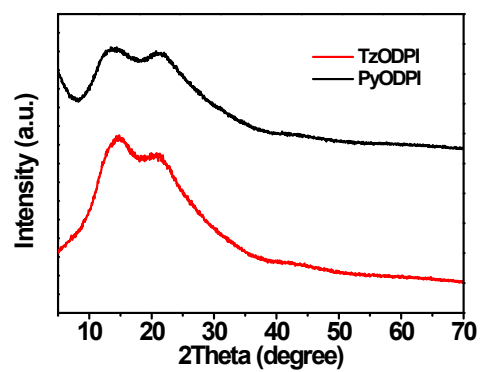


Fig. S5 WAXD patterns of the polyimide films

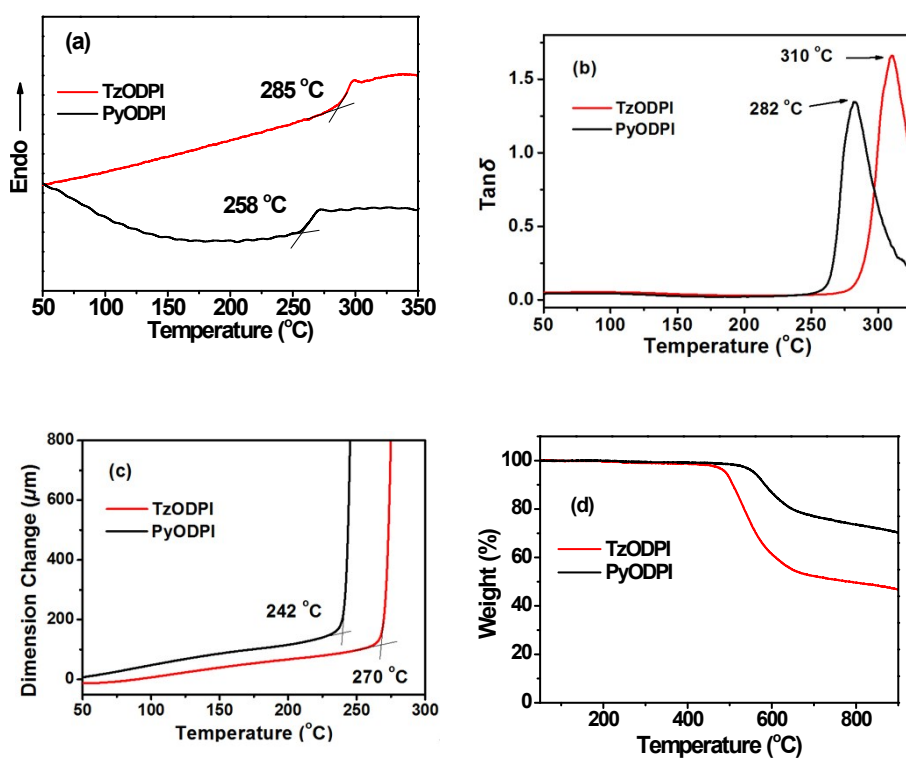


Fig. S6 Polyimides thermal properties: (a) DSC curves, (b) DMA curves, (c) TMA curves and (d) TGA curves

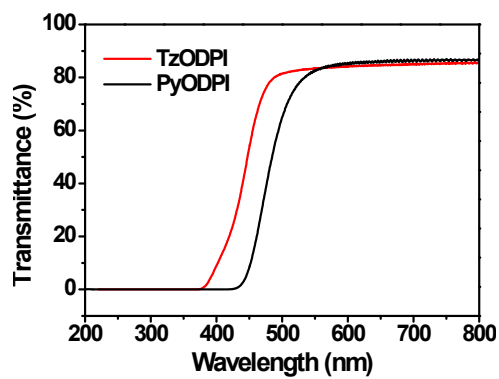


Fig. S7 Transmission spectra of polyimide films (ca. 35  $\mu\text{m}$ )

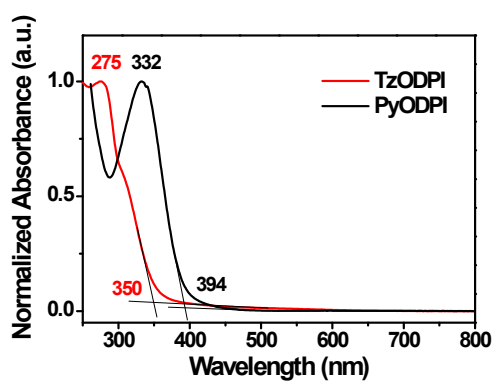


Fig. S8 Absorption spectra of polyimide spin-coated films

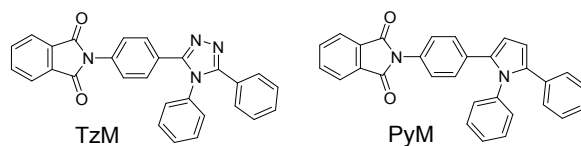


Fig. S9 The chemical structures of model basic units (MBU) TzM and PyM

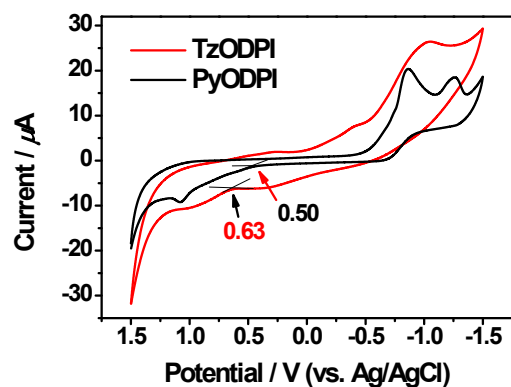


Fig. S10 Cyclic Voltammograms of polyimides in NMP